Synthesis and characterization of 1,2,3,4-naphthalene and anthracene diimides

Adam D. Bass, Daniela Castellanos, Xavier A. Calicdan and Dennis D. Cao*

Full Research Paper

Address:

Chemistry Department, Macalester College, 1600 Grand Avenue, Saint Paul, Minnesota 55105, United States

Email

Dennis D. Cao* - dcao@macalester.edu

* Corresponding author

Keywords:

electron acceptors; organic materials; polycyclic aromatic hydrocarbons

Beilstein J. Org. Chem. **2024**, *20*, 1767–1772. https://doi.org/10.3762/bjoc.20.155

Received: 18 March 2024 Accepted: 11 July 2024 Published: 25 July 2024

This article is part of the thematic issue " π -Conjugated molecules and

naterials".

Guest Editor: A. Mateo-Alonso



© 2024 Bass et al.; licensee Beilstein-Institut. License and terms: see end of document.

Open Access

Abstract

We report the synthesis and characterization of naphthalene and anthracene scaffolds end-capped by cyclic imides. The solid-state structures of the *N*-phenyl derivatives, determined by X-ray crystallography, reveal changes in packing preference based on the number of aromatic rings in the core. The optical and electronic properties of the title compounds compare favorably with other previously described isomers and expand the toolbox of electron-deficient aromatic compounds available to organic materials chemists.

Introduction

Aromatic diimides are ubiquitous molecular scaffolds that have served as the basis for robust polymers, supramolecular assemblies, and (opto)electronic materials. The vast majority of this research has focused on 1,2,4,5-benzene (pyromellitic), 1,4,5,8-naphthalene, and 3,4,9,10-perylene diimides. Beyond these, researchers have demonstrated that translocating the cyclic imides around the periphery of the aromatic core to yield different structural isomers is effective for producing interesting new materials. Ourselves and others have investigated 1,2,3,4-benzene diimide, also known as mellophanic diimide [1], as a building block for heteroacenes [2-5] and polyimides [6-8]. The

1,2,5,6- [9,10] and 2,3,6,7-naphthalene diimides (NDIs) have been produced and utilized in electronically active polymers (Figure 1). The linear extension of 1,4,5,8-naphthalene diimide to produce tetracene [11] and hexacene [12] diimides, some with interesting properties such as near-IR absorption, has been achieved as well. Other efforts have demonstrated that anthracene diimides (ADIs) can be tuned to achieve decent electron mobilities in electronic settings [13,14]. Although there have been calculations conducted that suggest 6-membered cyclic imides are more compelling than 5-membered cyclic imides in organic electronic materials [15], the experimental ob-

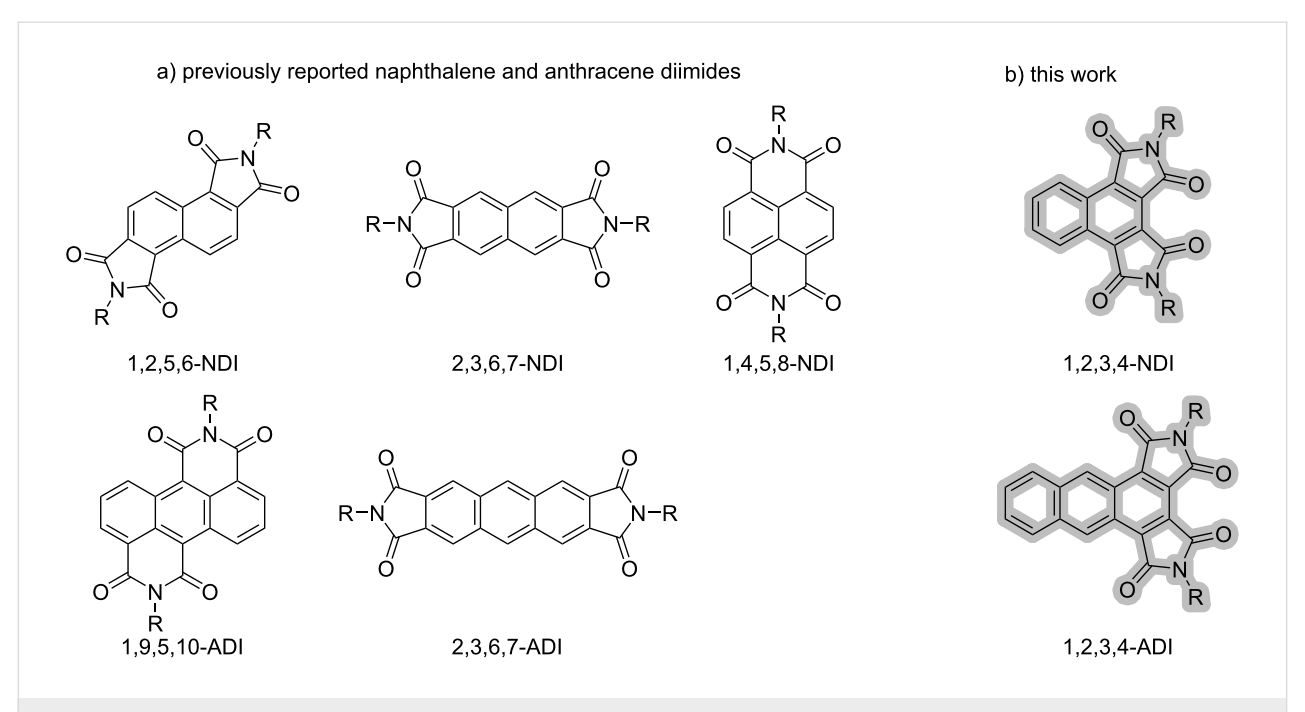


Figure 1: a) Structures of previously reported naphthalene and anthracene diimide isomers. b) The novel 1,2,3,4-naphthalene and -anthracene diimides reported here.

servation of similar electron mobilities across different structural isomers of naphthalene and anthracene diimide [16] confirms the need to experimentally evaluate the unstudied isomers.

We became interested in the *cata*- (i.e. 1,2,3,4-) derivatization of aromatic scaffolds because it can be exploited to stabilize the longer (hetero)acenes. In contrast to *cata*-benzannulation, *cata*-imide-annulation does not perturb aromaticity patterns and further introduces inductive stabilization of frontier MO levels, which has enabled the production of n-type organic thin-film transistors from heteroacenes. Inspired by these results, we sought to demonstrate the preparation of all-carbon scaffolds, i.e., acenes, that are *cata*-annulated with cyclic imides. Here, we communicate the successful synthesis of 1,2,3,4-NDIs and -ADIs and the characterization of their physical properties.

Results and Discussion Synthesis

The synthesis of the title compounds is shown in Scheme 1. To obtain a naphthalene core with the requisite 1,2,3,4-tetracarbonyl derivatization pattern, we leveraged the cycloaddition of 1 equiv of aryne percursor 1 with 2 equiv of dimethyl acetylenedicarboxylate (DMAD). Although this [2 + 2 + 2] cycloaddition reactivity strategy has been reported under a variety of aryne generation conditions [17-19], in our hands we were only able to generate practical amounts of tetraesters 3 using the method reported by Peña et al. [18]. Hydrolysis of 3

with sodium hydroxide, followed by acidification with HCl, yielded a mixture of carboxylic acids and anhydrides **5**, as evidenced by ¹H NMR spectroscopy (Figure S13 in Supporting Information File 1). Gratifyingly, purification of these mixtures was not necessary as they could be used directly for imidization. Heating **5** with hexylamine or aniline in refluxing acetic acid successfully led to the formation of the targeted aromatic diimides bearing either *N*-hexyl (**7-Hex**) or *N*-phenyl (**7-Ph**) substitutions in good yields. The same strategy was employed to create the imide-capped anthracenes **8-Hex** and **8-Ph**.

Crystallography

Despite exhaustive efforts, we were unable to obtain single crystals of 7-Hex and 8-Hex; these compounds formed polycrystalline bundles that are fragile and insufficient for obtaining diffraction data. Fortunately, single crystals of the N-phenyl compounds were successfully grown by slow evaporation of CH₂Cl₂/MeOH solutions and characterized by X-ray crystallography. **7-Ph** crystallizes in the *Pbcn* space group into a solvent superstructure of π -stacked columns of **7-Ph**. The imide groups are pointed in alternating directions within a stack. While this may occur in part as a consequence of the steric demands of the *N*-phenyl groups, there are also $C-H\cdots\pi$ interactions between phenyl groups of adjacent π stacks, with the closest Ph centroid to H distance being 2.613 Å (Figure 2a). Additionally, the middle carbonyl oxygens are in short contact (2.376 Å) with the 7- and 8-H atoms of the naphthalene in the adjacent molecule (Figure 2a).

 $\textbf{Scheme 1:} \ a) \ \text{Synthesis of the 1,2,3,4-naphthalene and -anthracene diimides. Conditions:} \ i) \ \text{CsF/Pd}_2(\text{dba})_3/\text{MeCN}; \ ii) \ \text{NaOH/H}_2\text{O/THF}, \ \text{then HCl}; \ iii) \ \text{R-NH}_2/\text{AcOH.} \ b) \ \text{X-ray crystal structures of 7-Ph} \ \text{and 8-Ph}.$

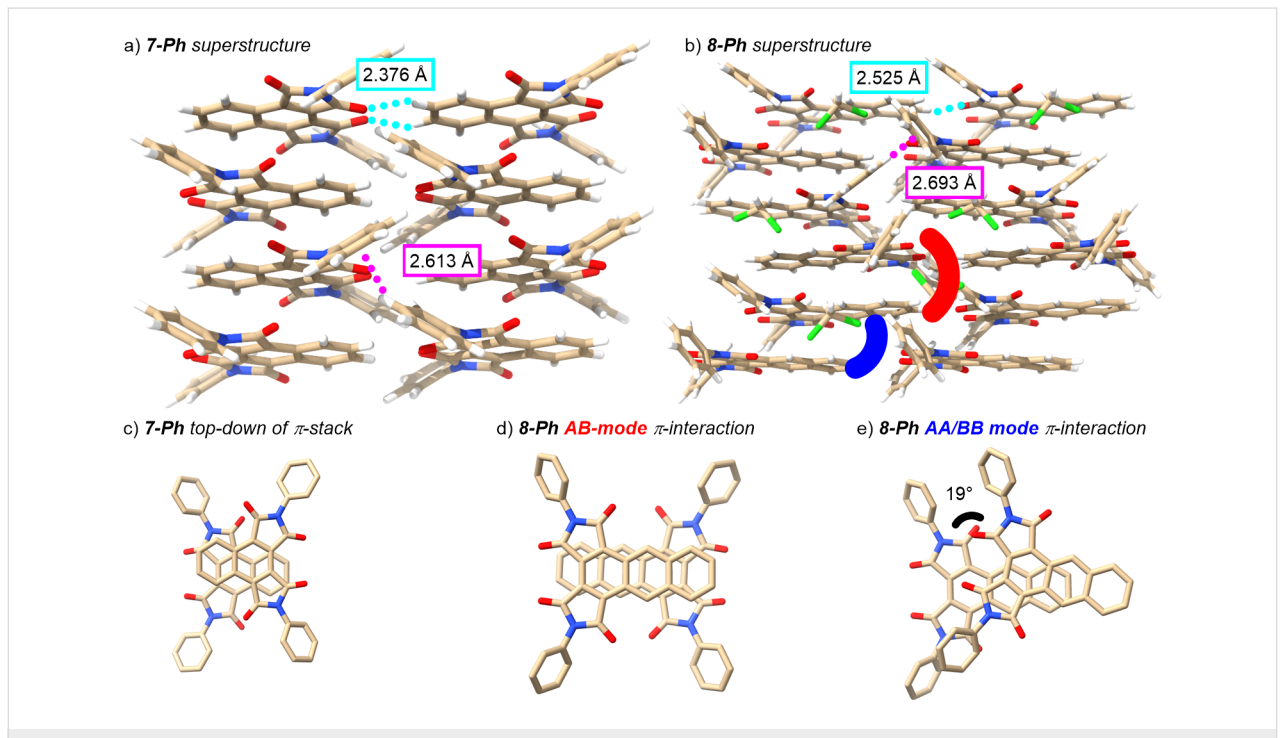


Figure 2: Superstructures for a) 7-Ph and b) 8-Ph as determined by X-ray crystallography. Representative $C=O\cdots H-C$ and $C-H\cdots \pi$ interactions are indicated in teal and magenta, respectively. Top-down views of π -stacking modes in c) 7-Ph and d, e) 8-Ph. Hydrogen atoms have been removed for clarity in c–e. Atom color code: $C = \tan \theta$, H = white, CI = green, N = blue, and O = red.

On the other hand, **8-Ph** crystallizes in the *Pbca* space group with two molecules of interest along with one molecule of CH_2Cl_2 . Pairs of **8-Ph** molecules are π -stacked together with their imide groups oriented in opposing directions (Figure 2d)

in a fashion analogous to that observed for **7-Ph** (Figure 2c). These pairs, however, are then infinitely packed such that adjacent **8-Ph** molecules are aligned in the same direction to create an AA-BB stacking pattern, unlike the more common

A–B–A–B stacking pattern found for **7-Ph**. Additionally, it is worth observing that the π -interaction involving two **8-Ph** molecules pointed in the same nominal direction is not linearly aligned, but is instead twisted by 19°. This angle, likely enforced by the sterics of the phenyl groups, may be an interesting approach to inducing helical turns in supramolecular assemblies derived from the title compounds.

Despite this different packing mode within the stack, the interstack interactions exhibited by **8-Ph** are similar to those found in **7-Ph**. Although there are still observable $C-H\cdots\pi$ interactions and $C=O\cdots H-C$ interactions between stacks, they appear to be weaker, as evidenced by the longer interaction distances and interceding incorporation of CH_2Cl_2 (Figure 2b). Furthermore, in **8-Ph** the interstack $C=O\cdots H-C$ interaction is skewed such as to involve only one C=O, compared to the symmetric dual-contact that is seen for **7-Ph**.

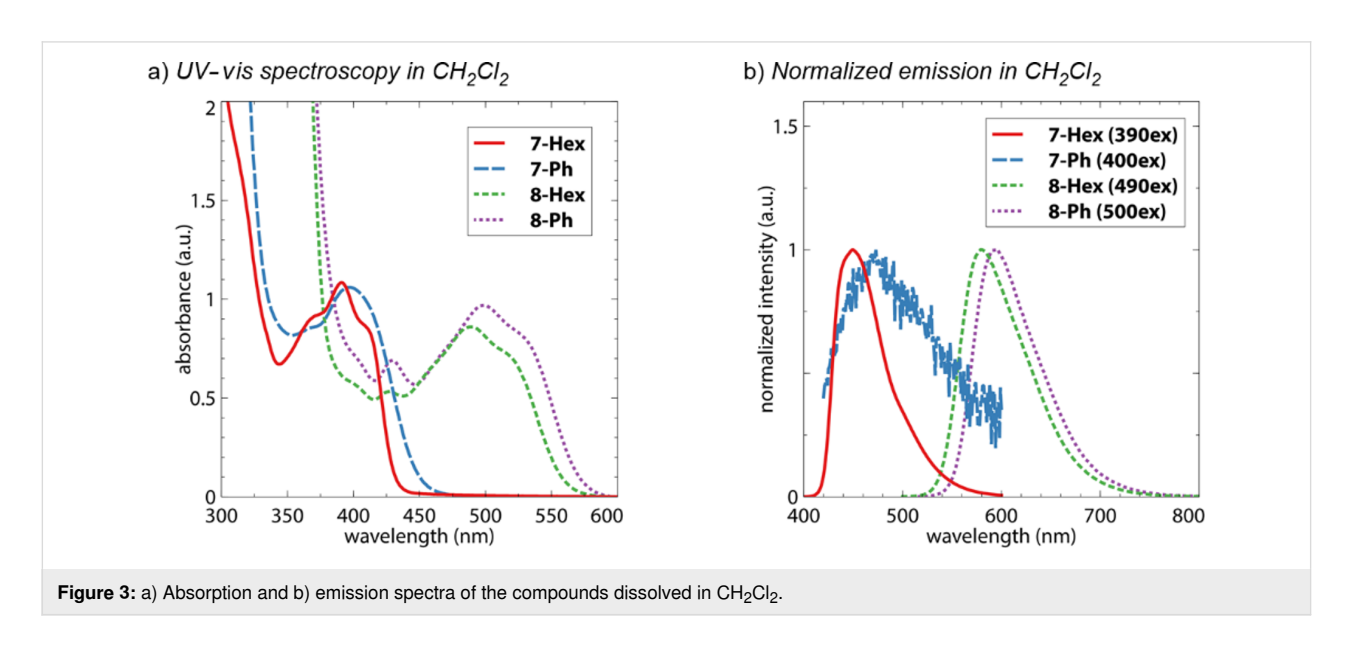
Optical and electronic characterization

The absorption spectra of the diimides dissolved in CH_2Cl_2 are depicted in Figure 3a. All of these compounds exhibit broad absorption bands. **7-Hex** has more well-defined features with $\lambda_{max} = 391$ nm while **7-Ph** has a slightly longer wavelength absorption with $\lambda_{max} = 398$ nm. A similar trend is observed for **8-Hex** and **8-Ph**, with $\lambda_{max} = 489$ and 499 nm, respectively. These absorption features are roughly comparable to other naphthalene and anthracene diimides that have been reported in the literature. The emission profiles of all four compounds are shown in Figure 3b. While N,N'-dibutyl-1,4,5,8-naphthalene diimide has low fluorescence intensity ($\Phi = 0.006$) [20], **7-Hex** emits more efficiently with $\Phi = 0.41$. Interestingly, **7-Ph** has nearly no emission intensity, as evidenced by the low signal-tonoise ratio in the data and a near-zero quantum yield when

excited at 400 nm. This fluorescence quenching is likely related to non-radiative emission that is observed for *N*-phenyl-substituted imides [21]. It is possible this effect is more significant for **7-Ph** than **8-Ph** because the naphthalene core is less conformationally locked than the anthracene scaffold.

As is expected for aromatic diimides, the title compounds undergo reversible chemical reduction processes, as determined by cyclic voltammetry in CH₂Cl₂ solvent (Figure 4). There are two factors at play. The imide substitution is impactful as the N-phenyl derivatives are roughly by 100 mV easier to reduce than the N-hexyl analogs. The anthracene scaffold also lends itself to a more facile reduction process, with an approximately 150 mV shift of the event toward more positive potentials for 8-R vs 7-R. When compared to other structural isomers, aromatic diimides with 5-membered cyclic imides tend to be slightly harder to reduce than those with 6-membered cyclic imides (Table 1). Overall, however, the cata-annulation does not lead to substantially different electrochemical behavior, which is encouraging because we had anticipated that the deflection away from planarity caused by adjacent placement of cyclic imides might adversely affect extent of π -delocalization.

As part of our previous work constructing heteroacenes bearing *cata*-imide groups, we investigated the 9,10-diaza analog of compound **8-Hex** (**9**, Figure 5). It is interesting to note that the all-carbon scaffold in **8-Hex** results in a narrower bandgap than that of **9**, with $\Delta\lambda_{max} = 85$ nm. This difference can be attributed to a significantly higher HOMO level in **8-Hex** arising from having fewer electronegative atoms in the aromatic backbone. For the same reasons, compound **9** is a superior electron acceptor by 0.36 V. These trends confirm the value of backbone atom substitution for fine-tuning molecular properties.



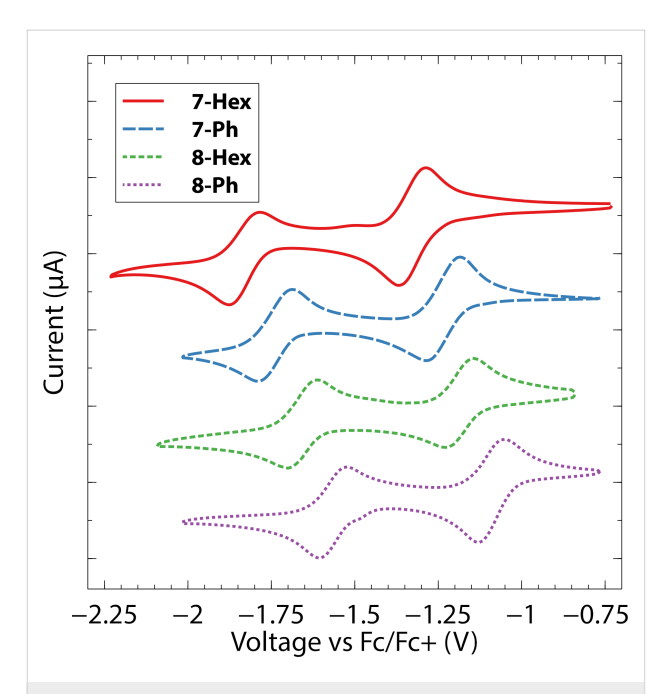


Figure 4: Cyclic voltammograms of the compounds collected on ca. 1 mM solutions of the analyte in CH_2CI_2 with 0.1 M Bu_4NPF_6 as electrolyte. The major *y*-axis tick mark spacing corresponds to 5 μ A.

Figure 5: Structural formula of 9, the diaza-analog of compound 8-Hex that was reported previously [2].

Conclusion

In conclusion, we have demonstrated the facile construction of two new aromatic diimide scaffolds: 1,2,3,4-naphthalene and -anthracene diimides through a cycloaddition approach to construct the aromatic backbone prior to imide formation. The physical characterization of the title compounds indicates that they are optically and electronically similar to previously reported naphthalene and anthracene diimides, absorbing/emitting light in the visible region and readily undergoing one-electron-reduction processes. As such, this work opens the possibility of incorporating the 1,2,3,4-naphthalene and -anthracene diimide motifs as productive building blocks in imide-based organic materials.

Supporting Information

Supporting Information File 1

Experimental procedures, synthetic protocols, and X-ray crystallographic data.

[https://www.beilstein-journals.org/bjoc/content/supplementary/1860-5397-20-155-S1.pdf]

Supporting Information File 2

Crystallographic information file for compound **7-Ph**. [https://www.beilstein-journals.org/bjoc/content/supplementary/1860-5397-20-155-S2.cif]

Supporting Information File 3

Crystallographic information file for compound **8-Ph**. [https://www.beilstein-journals.org/bjoc/content/supplementary/1860-5397-20-155-S3.cif]

| Table 1: Summary and comparison of optical and electronic properties. |
|--|
|--|

| | E_{V_2} (V vs Fc/Fc ⁺) ^a | | | | | | | |
|--------------------------------|---|---------------------|----------------------------|-------------------------|-------------------------|---------------------------|---------------------------|------------|
| | E _{2r} (V) | E _{1r} (V) | λ _{max} b (nm) | λ _{em} (nm) | Eg ^c (eV) | LUMO ^d (eV) | HOMO ^e (eV) | Φ |
| 7-Hex | -1.83 | -1.33 | 391 | 450 | 2.82 | -3.5 | -6.3 | 0.41 |
| 7-Ph | -1.74 | -1.23 | 398 | 519 ^f | 2.64 | -3.6 | -6.2 | <0.01 |
| 1,2,5,6-NDI [9] | | -1.20 ^g | | | | -3.6 | | |
| 1,4,5,8-NDI [22] | -1.51 | -1.10 | 370 | | 3.18 | -3.7 | -6.9 | 0.006 [20] |
| 8-Hex | -1.66 | -1.19 | 489 | 575 | 2.15 | -3.6 | -5.7 | 0.20 |
| 8-Ph | -1.56 | -1.09 | 498 | 595 | 2.07 | -3.5 | -5.6 | 0.04 |
| 1,9,5,10-ADI ^h [14] | -1.40 ^g | -1.10 ^g | 480 | 525 | 2.2 | -3.8 | -6.0 | |
| 2,3,6,7-ADI [13] | | -1.69 | | | | | | |
| 9 [2] | -1.30 | -0.76 | 404 | | 2.56 | -4.2 | -6.8 | |

 $^{\mathrm{q}}$ Unless otherwise noted, ca. 1 mM analyte in CH2Cl2, 0.1 M Bu4NPF₆. $^{\mathrm{b}}$ Unless otherwise noted, longest wavelength absorption maxima of analyte in CH2Cl2 solution. $^{\mathrm{c}}$ Optical bandgap estimated from absorption onset. $^{\mathrm{d}}$ LUMO estimated from reduction onset. $^{\mathrm{e}}$ HOMO = LUMO – E_{g} . $^{\mathrm{f}}$ Low intensity emission. $^{\mathrm{g}}$ Estimated from graphical data. $^{\mathrm{h}}$ PhCl solvent.

Acknowledgements

We thank Victor G. Young, Jr. of the University of Minnesota X-Ray Crystallographic Laboratory for acquiring X-ray diffraction data and solving crystal structures.

Funding

The Bruker-AXS D8 Venture diffractometer was purchased through a grant from NSF/MRI (#1229400) and the University of Minnesota. This work was additionally supported by the National Science Foundation under Grant No. NSF 1954975 and the Beckman Foundation Beckman Scholars Program.

ORCID® iDs

Adam D. Bass - https://orcid.org/0000-0003-2899-0686 Dennis D. Cao - https://orcid.org/0000-0002-0315-1619

Data Availability Statement

All data that supports the findings of this study is available in the published article and/or the supporting information to this article.

References

- Zou, B.; Stellmach, K. A.; Luo, S. M.; Gebresilassie, F. L.; Jung, H.; Zhang, C. K.; Bass, A. D.; Janzen, D. E.; Cao, D. D. J. Org. Chem. 2022, 87, 13605–13614. doi:10.1021/acs.joc.2c01241
- Luo, S. M.; Stellmach, K. A.; Ikuzwe, S. M.; Cao, D. D. J. Org. Chem. 2019, 84, 10362–10370. doi:10.1021/acs.joc.9b01502
- Elter, M.; Ahrens, L.; Luo, S. M.; Rominger, F.; Freudenberg, J.;
 Cao, D. D.; Bunz, U. H. F. Chem. Eur. J. 2021, 27, 12284–12288.
 doi:10.1002/chem.202101573
- Hippchen, N.; Heinzel, E.; Zhang, C. K.; Jäger, P.; Elter, M.; Ludwig, P.; Rominger, F.; Freudenberg, J.; Cao, D. D.; Bunz, U. H. F. ChemPlusChem 2023, 88, e202300158. doi:10.1002/cplu.202300158
- Yi, X.; Gao, J.; Qin, H.; Zheng, L.; Zeng, W.; Chen, H. Org. Lett. 2023, 25, 972–976. doi:10.1021/acs.orglett.3c00001
- Fang, X.; Yang, Z.; Zhang, S.; Gao, L.; Ding, M. Macromolecules 2002, 35, 8708–8717. doi:10.1021/ma0204610
- Hasegawa, M.; Nomura, R. React. Funct. Polym. 2011, 71, 109–120. doi:10.1016/j.reactfunctpolym.2010.11.021
- Zhao, L.; Li, W.; Qin, H.; Yi, X.; Zeng, W.; Zhao, Y.; Chen, H. *Macromolecules* 2023, 56, 2990–3003. doi:10.1021/acs.macromol.3c00252
- Chen, S.-c.; Zhang, Q.; Zheng, Q.; Tang, C.; Lu, C.-Z. Chem. Commun. 2012, 48, 1254–1256. doi:10.1039/c2cc15733k
- Zhao, Z.; Zhang, F.; Zhang, X.; Yang, X.; Li, H.; Gao, X.; Di, C.-a.;
 Zhu, D. *Macromolecules* 2013, 46, 7705–7714.
 doi:10.1021/ma4013994
- 11. Yue, W.; Gao, J.; Li, Y.; Jiang, W.; Di Motta, S.; Negri, F.; Wang, Z. J. Am. Chem. Soc. **2011**, *133*, 18054–18057. doi:10.1021/ja207630a
- Cui, X.; Xiao, C.; Winands, T.; Koch, T.; Li, Y.; Zhang, L.;
 Doltsinis, N. L.; Wang, Z. J. Am. Chem. Soc. 2018, 140, 12175–12180.
 doi:10.1021/jacs.8b07305
- Wang, Z.; Kim, C.; Facchetti, A.; Marks, T. J. J. Am. Chem. Soc. 2007, 129, 13362–13363. doi:10.1021/ja073306f
- Mohebbi, A. R.; Munoz, C.; Wudl, F. Org. Lett. 2011, 13, 2560–2563. doi:10.1021/ol200659c

- Chen, X.-K.; Zou, L.-Y.; Guo, J.-F.; Ren, A.-M. J. Mater. Chem. 2012, 22, 6471–6484. doi:10.1039/c2jm15935j
- Zhan, X.; Facchetti, A.; Barlow, S.; Marks, T. J.; Ratner, M. A.;
 Wasielewski, M. R.; Marder, S. R. Adv. Mater. (Weinheim, Ger.) 2011,
 23, 268–284. doi:10.1002/adma.201001402
- Hsieh, J.-C.; Cheng, C.-H. Chem. Commun. 2008, 2992–2994. doi:10.1039/b801870g
- Peña, D.; Pérez, D.; Guitián, E.; Castedo, L. J. Org. Chem. 2000, 65, 6944–6950. doi:10.1021/jo000535a
- 19. Jafarpour, F.; Hazrati, H.; Nouraldinmousa, S. *Org. Lett.* **2013**, *15*, 3816–3819. doi:10.1021/ol401318v
- Maniam, S.; Higginbotham, H. F.; Bell, T. D. M.; Langford, S. J.
 Chem. Eur. J. 2019, 25, 7044–7057. doi:10.1002/chem.201806008
- Demeter, A.; Bérces, T.; Biczók, L.; Wintgens, V.; Valat, P.; Kossanyi, J. J. Phys. Chem. 1996, 100, 2001–2011. doi:10.1021/jp951133n
- 22. Thalacker, C.; Röger, C.; Würthner, F. J. Org. Chem. **2006**, *71*, 8098–8105. doi:10.1021/jo0612269

License and Terms

This is an open access article licensed under the terms of the Beilstein-Institut Open Access License Agreement (https://www.beilstein-journals.org/bjoc/terms), which is identical to the Creative Commons Attribution 4.0 International License

(https://creativecommons.org/licenses/by/4.0). The reuse of material under this license requires that the author(s), source and license are credited. Third-party material in this article could be subject to other licenses (typically indicated in the credit line), and in this case, users are required to obtain permission from the license holder to reuse the material.

The definitive version of this article is the electronic one which can be found at:

https://doi.org/10.3762/bjoc.20.155